

# Preparation and Adsorption Properties of Microporous Manganese Titanate Pillared with Silica

Shoji Yamanaka,<sup>\*,†,‡</sup> Katsuyuki Kunii,<sup>†</sup> and Zhang-Lin Xu<sup>†</sup>

Department of Applied Chemistry, Faculty of Engineering, Hiroshima University, Higashi-hiroshima 739-8527, Japan, and CREST, Japan Science and Technology Corporation (JST), Japan

Received February 23, 1998. Revised Manuscript Received April 20, 1998

The layered material  $\text{Rb}_x\text{Mn}_x\text{Ti}_{2-x}\text{O}_4$  ( $x = 0.75$ ) was pillared with silica. The Rb ions were first exchanged with  $n$ -alkylammonium ions ( $\text{C}_n\text{H}_{2n+1}\text{NH}_3$ ,  $n = 6-18$ ) to separate the interlayer space of the titanate, and then tetraethoxysilane was hydrolyzed between the layers. Burning off the organic parts resulted in silica pillared microporous solids with a surface area as large as 500–800  $\text{m}^2/\text{g}$ . The porous structure was stable up to 600 °C. Adsorption–desorption isotherms for various vapors, such as water, methanol, toluene, and mesitylene, were measured, which suggested that the porous structure formed between the layers was very similar to those of zeolites and uniform without mesopores. The pores showed hydrophobic properties. Their size was on the order of that of mesitylene.

## Introduction

According to the classification of IUPAC (the International Union of Pure and Applied Chemistry),<sup>1</sup> pores in solids are classified into three categories by their width ( $w$ ): micropores with  $w < \sim 2$  nm, mesopores with  $\sim 2$  nm  $< w < \sim 50$  nm, and macropores with  $w > \sim 50$  nm. Most of pores are made in the interstices of aggregates composed of particles of a powder. The pores of silica gels, for example, are formed in the interstices surrounded by silica sol particles,<sup>2</sup> the pore sizes being dependent on the size of sol particles. The pores in silica gels are mainly mesopores. Although the pore size decreases with the decrease of the size of the sol particles, there is a lower limit of the pore size attainable. Even if the size of the sol particles could be so small as to form microporous aggregates, the sol particles would rather form a solid mass without pores. Microporous solids so far known had been crystals in which the micropores are included as a part of the crystal structure, such as zeolites. Pillared clays are a new type of microporous materials, where the silicate layers of clays with a thickness on the molecular level are pillared with ceramic oxide particles with nano- to subnanometer sizes,<sup>3–5</sup> such as  $\text{Al}_2\text{O}_3$ ,<sup>6</sup>  $\text{ZrO}_2$ ,<sup>7</sup>  $\text{Cr}_2\text{O}_3$ ,<sup>8,9</sup>  $\text{TiO}_2$ ,<sup>10,11</sup>  $\text{Fe}_2\text{O}_3$ ,<sup>12,13</sup> and  $\text{SiO}_2$ .<sup>14,15</sup> The ceramic oxide

particles keep the silicate layers apart and form micropores corresponding to the size of the particles. The significance of the success in the development of pillared clays is demonstrated by the new type of microporous solids other than zeolites that have been synthesized for the first time.<sup>16</sup> However, zeolites and pillared clays with silicate networks are insulators. Recently, a variety of nonclay pillared materials have also been derived from metal phosphates and layered double hydroxides.<sup>17–19</sup> Those are still composed of insulating host layers. Micropores with semiconducting or metallic networks should be developed in the next stage.

There are a number of transition metal oxides and oxyanions that are interesting candidates for host layers to pillar with semiconducting properties. Pillared clays are usually prepared by the ion-exchange of the cations between the silicate layers of clays with bulky hydroxymetal cations such as  $[\text{Al}_{13}\text{O}_4(\text{OH})_{13}]^{7+}$  and  $[\text{Zr}_4(\text{OH})_{14}]^{2+}$ , which are then converted to the oxide pillars on heating. The intercalated oxide pillars prevent the interlayer spaces from collapse and result in stable microporous structures with high surface areas. Layered titanates were pillared with alumina and zirconia by an ion-

\* To whom correspondence should be addressed. Tel & Fax: 81-824-24-7740. E-mail: syamana@ipc.hiroshima-u.ac.jp.

† Hiroshima University.

‡ Japan Science and Technology Corporation.

(1) IUPAC Manual of Symbols and Terminology, Appendix 2, Pt. 1, Colloid and Surface Chemistry. *Pure Appl. Chem.* **1972**, *31*, 578.

(2) Iler, R. K. *The Chemistry of Silica*; John Wiley & Sons: New York, 1978; pp 174.

(3) Pinnavaia, T. J. *Science* **1983**, *220*, 365.

(4) Burch, R. *Catal. Today* **1988**, *2*, 185.

(5) Yamanaka, S.; Hattori, M. *Chemistry of Microporous Crystals*; Inui, T., Namba, S., Tatsumi, T., Eds.; Kodansha/Elsevier: Tokyo, 1991; pp 89.

(6) Brindley, G. W.; Sempels, R. E. *Clay Miner.* **1977**, *12*, 229.

(7) Yamanaka, S.; Brindley, G. W. *Clays Clay Miner.* **1979**, *27*, 119.

(8) Brindley, G. W.; Yamanaka, S. *Am. Miner.* **1979**, *64*, 830.

(9) Pinnavaia, T. J.; Tzou, M. S.; Landau, S. D. *J. Am. Chem. Soc.* **1985**, *107*, 783.

(10) Yamanaka, S.; Nishihara, T.; Hattori, M.; Suzuki, Y. *Mater. Chem. Phys.* **1987**, *17*, 87.

(11) Yamanaka, S.; Makita, K. *J. Porous Mater.* **1995**, *1*, 29.

(12) Yamanaka, S.; Doi, T.; Sako, S.; Hattori, M. *Mater. Res. Bull.* **1984**, *19*, 161.

(13) Rightor, E. G.; Tzou, M. S.; Pinnavaia, T. J. *J. Catal.* **1991**, *130*, 29.

(14) Yamanaka, S.; Inoue, Y.; Hattori, M.; Okumura, F.; Yoshikawa, M. *Bull. Chem. Soc. Jpn.* **1992**, *65*, 2494.

(15) Han, Y.-S.; Matsumoto, H.; Yamanaka, S. *Chem. Mater.* **1997**, *9*, 2013.

(16) Yamanaka, S. *Am. Ceramic Soc. Bull.* **1991**, *70*, 1056.

(17) Clearfield, A. In *Multifunctional Mesoporous Inorganic Solids*; Sequeira, C. A. C., Hudson, M. J., Eds.; Kluwer Academic Publishers: Dordrecht, 1992; p 159.

(18) Corma, A. *Chem. Rev.* **1997**, *97*, 2373.

(19) Ohtsuka, K. *Chem. Mater.* **1997**, *9*, 2039.

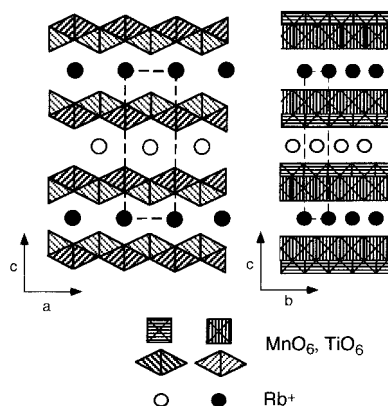


**Figure 1.** Schematic structural model of  $\text{Rb}_x\text{Mn}_x\text{Ti}_{2-x}\text{O}_4$  ( $x = 0.75$ ). The interlayer cation sites are partially filled with Rb ions.

exchange method similar to that used in the pillared clay synthesis.<sup>20,21</sup> However, the direct ion-exchange method cannot usually be applied to the pillaring of most of layered compounds, since most layered compounds do not swell like clays. Landis et al.<sup>22</sup> developed a new method, where the layered compounds were first intercalated with organic ammonium ions to increase the interlayer distance, and then silicon alkoxides were hydrolyzed between the layers. On burning off the organic material between the layers, silica pillared structures were obtained. A layered titanate,  $\text{Na}_2\text{-Ti}_3\text{O}_7$ ,<sup>22</sup> and a layered perovskite,  $\text{KCa}_2\text{Nb}_3\text{O}_{10}$ ,<sup>23</sup> were pillared with silica according to this method. In this study, an ion-exchangeable layer-structured manganese titanate,  $\text{Rb}_x\text{Mn}_x\text{Ti}_{2-x}\text{O}_4$  ( $x = 0.75$ ), hereafter called  $\text{Rb}_{0.75}\text{MTO}$ , has been synthesized and pillared with silica according to the procedure by Landis et al.<sup>22</sup> A schematic structural model of  $\text{Rb}_{0.75}\text{MTO}$  is given in Figure 1. It has a layered structure of  $\gamma\text{-FeO}(\text{OH})$  type,<sup>24</sup> where Mn(III) and Ti(IV) occupy the Fe sites and O occupy the O and (OH) sites. Rb ions are located between the layers, balancing the negative charge formed by the replacement of Ti(IV) with Mn(III). The interlayer cations are replaced with alkylammonium ions of different lengths and pillared with silica by the treatment with tetraethoxysilane. Microporous solids with extremely high surface areas and high thermal stability comparable to zeolites are obtained.

### Experimental Section

**Materials.**  $\text{Rb}_{0.75}\text{MTO}$  was prepared according to the procedure of Reid et al.;<sup>24</sup>  $\text{RbMnO}_4$  was first prepared by the reaction of  $\text{RbCl}$  and  $\text{KMnO}_4$ , and a constituent mixture of  $\text{RbMnO}_4$  and  $\text{TiO}_2$  was calcined at  $800\text{ }^\circ\text{C}$  for 15 h. The product was ground and calcined again at  $1000\text{ }^\circ\text{C}$  for 7 h.  $n$ -Alkylammonium chlorides,  $\text{C}_n\text{H}_{2n+1}\text{NH}_3\text{Cl}$  ( $n = 6\text{--}18$ ), were prepared by the titration of the respective amine solutions in ethanol with hydrochloric acid, followed by crystallization. Tetraethoxysilane (TEOS) was from Katayama Chemical and used as received.

(20) Cheng, S.; Wang, T.-C. *Inorg. Chem.* **1989**, *28*, 1283.

(21) Anderson, M. W.; Klinowski, J. *Inorg. Chem.* **1990**, *29*, 3260.

(22) Landis, M. E.; Aufdembrink, B. A.; Chu, P.; Johnson, I. D.; Kirker, G. W.; Rubin, M. K. *J. Am. Chem. Soc.* **1991**, *113*, 3189.

(23) Ebina, Y.; Tanaka, A.; Kondo, J. N.; Domen, K. *Chem. Mater.* **1996**, *8*, 2534.

(24) Reid, A. F.; Mumme, W. G.; Wadsley, A. D. *Acta Crystallogr.* **1968**, B24, 1228.

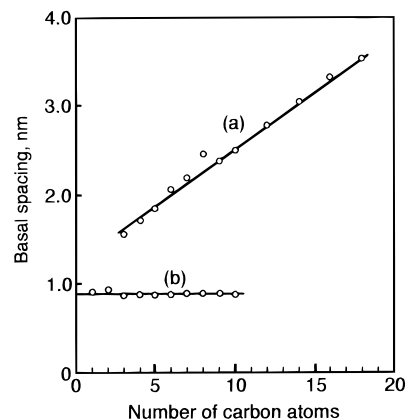


**Figure 2.** Basal spacing of  $A_n\text{-MTO}$  as a function of  $n$  (number of carbon atoms in the alkyl chains): (a) larger basal spacing compounds and (b) smaller basal spacing compounds.

**Pillaring with Silica.** The ion exchange of Rb ions with alkylammonium ions was carried out by dispersing  $\text{Rb}_{0.75}\text{MTO}$  (1 g) in the 0.1 M alkylammonium chloride aqueous solutions (100 mL) at  $80\text{ }^\circ\text{C}$ . The solutions were replaced three times during the 6-day reaction. After the reaction, the samples were washed with water and dried in a desiccator over silica gel. The samples intercalated with alkylammonium pillars, hereafter called  $A_n\text{-MTO}$ , where  $n$  is the number of carbon atoms in the alkyl chain, were in turn dispersed in excess TEOS (0.1 g of  $A_n\text{-MTO}$  in a 20 mL of TEOS) and kept for 2 days at  $80\text{ }^\circ\text{C}$ . The products were separated by filtration and washed with ethanol, followed by drying at  $50\text{ }^\circ\text{C}$  in air. The dried products will be referred to as  $(\text{TEOS})\cdot A_n\text{-MTO}$ .

**Analyses.** X-ray powder diffraction (XRD) patterns were measured by using graphite-monochromated  $\text{Cu-K}\alpha$  radiation. Nitrogen adsorption isotherms were measured at liquid nitrogen temperature by a homemade computer-controlled volumetric apparatus on the sample degassed at  $200\text{ }^\circ\text{C}$  for 3 h in a vacuum. Adsorption isotherms of various vapors, water, methanol, toluene, and mesitylene, were measured at  $25\text{ }^\circ\text{C}$  on a gravimetric apparatus constructed with a Cahn electric balance (model 1000). Chemical analysis was performed by using an inductively coupled plasma (ICP) spectrometer on the samples dissolved in a mixture of hydrochloric acid and nitric acid solutions. A small amount of hydrofluoric acid was added to the solution for the complete dissolution.

### Results

**X-ray Diffraction Studies.** A  $\text{Rb}_{0.75}\text{MTO}$  sample was prepared as a single-phase, and the XRD pattern was indexed on the basis of an orthorhombic cell with  $a = 0.3927\text{ nm}$ ,  $b = 0.2934\text{ nm}$ , and  $c = 1.5956\text{ nm}$ , which is in good agreement with the unit cell reported by Reid et al.<sup>24</sup> The basal spacing ( $d$ ) of  $\text{Rb}_{0.75}\text{MTO}$  ( $d = c/2 = 0.79\text{ nm}$ ) showed a systematic increase after the exchange with  $n$ -alkylammonium ions with an increasing number of carbon atoms (Figure 2). The slope of the linear relationship in the figure was  $0.130\text{ nm/CH}_2$ . If the alkyl chains of all-trans conformation were arranged perpendicular to the layers, the increment of the length is  $0.127\text{ nm/CH}_2$ , and the cross sectional area occupied by each chain is estimated to be  $0.183\text{ nm}^2$  from the packing density of the alkyl chains with an all-trans configuration in a polyethylene crystal.<sup>25</sup> The Rb contents that remained in the exchanged products were determined to be less than 5% of the initial content, and the exchanged amounts of alkylammonium ions were

(25) Swan, P. R. *J. Polym. Sci.* **1962**, *56*, 409.

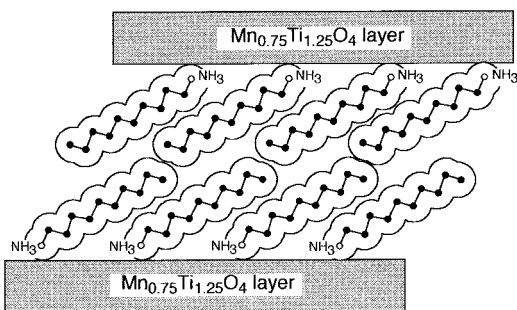


**Figure 3.** Schematic structural model of the arrangement of alkylammonium ions in bimolecular layers between the titanate layers. The alkyl chains in the all-trans configuration are inclined to the layers at an angle of ca. 31°.

estimated to be more than 95% of the total cation exchange capacity from the weight loss measured by thermogravimetric analysis. The maximum area available to the alkyl chain in monomolecular layers between the titanate layers was calculated to be ca. 0.15 nm<sup>2</sup> on the basis of the unit cell dimensions and the exchanged amount of alkylammonium ions. This area is much smaller than that required for the alkyl chain in monomolecular layers in A<sub>n</sub>-MTO. This suggests that the alkylammonium ions should be in bimolecular layers with inclination to the titanate layers at an angle of ca. 31°, as shown in Figure 3. Very similar arrangements of alkyl chains of ammonium ions between host layers were reported for clays<sup>26</sup> and a number of ion-exchangeable layered compounds.<sup>27,28</sup> In the initial stage of the ion exchange with *n*-alkylammonium ions, a basal spacing of 0.90 nm was observed (Figure 2, curve b). The spacing was not dependent on the length of the alkyl chains. This can be attributed to the arrangement of the alkyl chains parallel to the layers.

The basal spacings of A<sub>n</sub>-MTO further increased by the treatment with TEOS (Figure 4). The increase of the basal spacing suggested that TEOS molecules did intercalate into the interlayer space formed by the pillaring with alkyl chains. Although the spacing decreased on heating at 400 °C (Figure 4), it was much larger than that of the starting titanate. The A<sub>n</sub>-MTO samples contained about 7% water by weight. The TEOS molecules intercalated in A<sub>n</sub>-MTO would be hydrolyzed into silica precursors. If the A<sub>n</sub>-MTO samples were dried by heating at 100 °C for 1 day prior to the treatment with TEOS, the resulting products completely collapsed on heating at 400 °C. It is evident that the interlayer water molecules are essential for the formation of silica pillar precursors by interlamellar hydrolysis of TEOS.

**Adsorption Studies.** Figure 5 shows the changes of the basal spacing and the surface area of (TEOS)·A<sub>10</sub>-MTO on heating to 700 °C in air. The basal spacing decreased gradually from 3.1 to 2.0 nm on heating to 600 °C. The surface area showed a steep increase up to 800 m<sup>2</sup>/g at 300 °C with the decomposition of the organic parts and then decreased to 500 m<sup>2</sup>/g at 600 °C. The surface area began to decrease from 600 °C with a

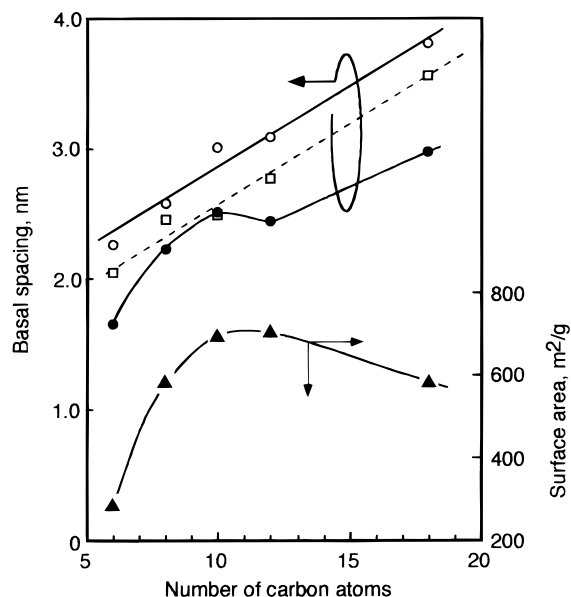


**Figure 4.** Basal spacing changes of A<sub>n</sub>-MTO as a function of *n* (number of carbon atoms) in the course of silica pillar formation: (□) A<sub>n</sub>-MTO, (○) (TEOS)·A<sub>n</sub>-MTO, and (●) SiO<sub>2</sub>-MTO obtained by calcination of (TEOS)·A<sub>n</sub>-MTO at 400 °C. The surface areas determined by nitrogen adsorption for the calcined samples (SiO<sub>2</sub>-MTO) are shown together (▲).

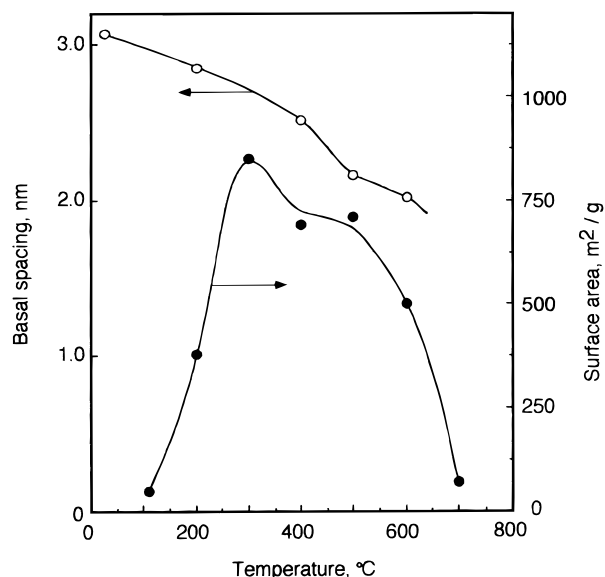


**Figure 5.** Basal spacing (○) and surface area (●) of (TEOS)·A<sub>10</sub>-MTO as a function of the calcination temperature.

slight decrease of the basal spacing. An abrupt decrease of the surface area at 700 °C was caused by the destruction of the pillared structures. Nitrogen adsorption-desorption isotherms were measured at liquid nitrogen temperature for the SiO<sub>2</sub>-MTO (*n* = 6–18) samples, which were derived from (TEOS)·A<sub>n</sub>-MTO (*n* = 6–18) by calcination at 400 °C, respectively. The results are shown in Figure 6. All isotherms are of typical type I (Langmuir type) for microporous solids and showed little hysteresis, suggesting that the pore structure is very uniform, like zeolites without mesopores. The Langmuir surface areas determined from the adsorption isotherms showed a tendency to increase with the increase of the basal spacing of SiO<sub>2</sub>-MTO, except the sample derived from (TEOS)·A<sub>18</sub>-MTO (Figure 4).

(26) Weiss, A. *Angew. Chem.* **1963**, 75, 113.

(27) Ertem, G.; Lagaly, G. *J. Colloid Interface Sci.* **1978**, 66, 12.

(28) Yamanaka, S.; Matsunaga, M.; Hattori, M. *J. Inorg. Nucl. Chem.* **1981**, 43, 1343.



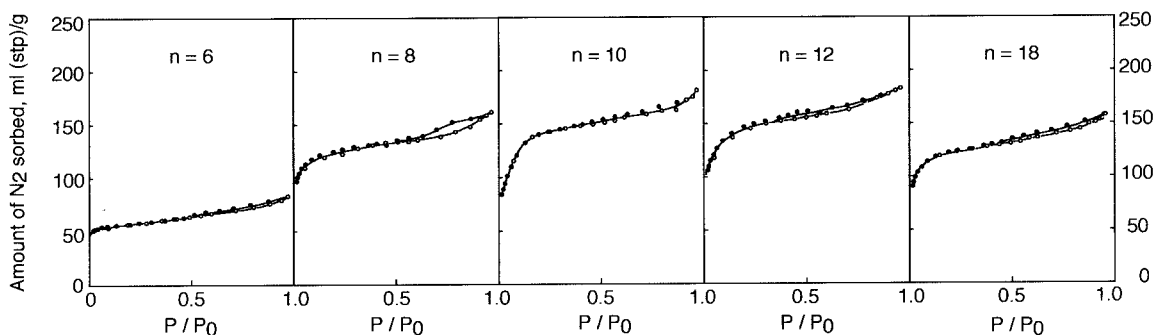


**Figure 6.** Nitrogen adsorption (○)–desorption (●) isotherms of SiO<sub>2</sub>-MTO obtained by using different lengths of alkylammonium ions and calcined at 400 °C. The number of carbon atoms (*n*) in the alkyl chains are shown in the figure.

Adsorption–desorption isotherms for various vapors, water, methanol, toluene, and mesitylene, are shown in Figure 7 on the SiO<sub>2</sub>-MTO (*n* = 6–18) samples. It is interesting to note that the sample obtained from (TEOS)·A<sub>6</sub>-MTO showed shape selectivity; the adsorption capacities for toluene and mesitylene were much reduced compared with those for smaller molecules such as water and methanol. This selectivity can be attributed to the smaller basal spacing of SiO<sub>2</sub>-MTO (*n* = 6). The rest of the samples with larger basal spacings did not show such a selectivity, but the isotherms obeyed the Gurvitch rule;<sup>29</sup> the total adsorption capacity (liquid volume) was almost the same irrespective of the size of adsorbates on the same adsorbent.

The isotherms for water and toluene indicated the pores to be hydrophobic; the adsorption of water in the very early stage of adsorption was rather gradual, in contrast to the steep increase in the adsorption of toluene. Similar hydrophobic properties were also observed in pillared clays,<sup>14,30</sup> where the interlayer cations were similarly exchanged with oxide pillars. Methanol-containing hydrophilic and hydrophobic parts in the same molecules had the isotherms with the shape between those of toluene and water. It should be noted that the adsorption–desorption isotherms for mesitylene showed a large hysteresis and adsorption required a threshold pressure. The threshold pressure showed a tendency to decrease with the increase of the alkyl chain length. This results from steric hindrance of the mesitylene in pore sizes similar to the dimensions of mesitylene.

**Chemical Analysis and Scanning Electron Microscopy (SEM).** The chemical analysis data of SiO<sub>2</sub>-MTO calcined at 900 °C are listed in Table 1. The silica content generally increased with the increase of the carbon number of the alkylammonium ions used. The Mn/Ti ratio after the pillaring decreased from 0.57 to 0.51–0.53. Although the reason for the loss or the dissolution of Mn from the host structure is not clear, the composition of the titanate layer is almost maintained before and after pillaring. The small surface area of the SiO<sub>2</sub>-MTO (*n* = 18) corresponds to the low silica content. As mentioned in the foregoing paragraph, the presence of interlayer water is essential for the formation of silica pillar precursors by the hydrolysis of TEOS. The amount of water contained in A<sub>18</sub>-MTO might be

**Table 1. Chemical Analysis Data of SiO<sub>2</sub>-MTO Prepared by Using Different Alkylammonium Ions**

<i>n</i>	wt %				atomic ratio		
	Rb <sub>2</sub> O	SiO <sub>2</sub>	Mn <sub>2</sub> O <sub>3</sub>	TiO <sub>2</sub>	total	Mn/Ti	Si/(Mn + Ti)
	Rb <sub>0.75</sub> MTO						
	30.0		25.0	44.6	99.6	0.57	
	SiO <sub>2</sub> -MTO						
6	1.3	28.9	22.9	45.3	98.4	0.51	0.56
8	0.1	33.8	22.4	43.4	99.7	0.52	0.68
10	0.0	35.4	22.3	43.4	101.1	0.52	0.71
12	0.0	40.4	19.4	38.2	98.0	0.51	0.93
18	0.1	33.9	21.5	41.1	96.6	0.53	0.72

not sufficient for the full development of stable pillars between the layers.

SEM photographs in Figure 8 of (TEOS)·A<sub>*n*</sub>-MTO before and after the calcination at 400 °C show that silica was not deposited on the external surface, and the crystal shape was maintained by pillaring.

The microporosity of SiO<sub>2</sub>-MTO was estimated from the increase of the unit cell volume ( $\Delta V$ ) and the volume of silica ( $V_{\text{SiO}_2}$ ) intercalated between the layers. The density of silica pillar was assumed to be cristobalite-like. The average layer thickness of MTO is 0.75 nm. The unit cell used for the calculation was a half of the unit cell shown in Figure 1;  $a \times b \times c/2$ . Since we know the compositions of SiO<sub>2</sub>-MTOs from Table 1, the nitrogen adsorption capacity (in mL/g) can be converted into the volume on the unit cell basis ( $V_{\text{pore}}$  in nm<sup>3</sup>/unit cell). The increase of the unit cell volume ( $\Delta V$ ) by the pillaring and the volumes of the intercalated silica ( $V_{\text{SiO}_2}$ ) plus micropores ( $V_{\text{pore}}$ ) thus determined are compared in Figure 9.  $\Delta V$  and ( $V_{\text{pore}} + V_{\text{SiO}_2}$ ) are in good agreement, except for the sample SiO<sub>2</sub>-MTO (*n* = 18). This suggests that all of the silica was effectively used to form micropores between the layers. If the silica is used to plug the pores between the layers, ( $V_{\text{pore}} + V_{\text{SiO}_2}$ ) would be smaller than  $\Delta V$ . On the contrary, if a large portion of the silica is deposited onto the external surface, ( $V_{\text{pore}} + V_{\text{SiO}_2}$ ) would be larger than  $\Delta V$ . Although the reason for the discrepancy of the total capacity from  $\Delta V$  for SiO<sub>2</sub>-MTO (*n* = 18) is not clear, it might be caused by the former case.

## Discussion

SiO<sub>2</sub>-MTO obtained in this study has the largest surface area and highest thermal stability among non-silicate pillared materials ever prepared. Although the mechanism of pillar formation will be studied in more detail, it is apparent that silica pillar precursors are

(29) Gurvitch, L. *J. Phys. Chem. Soc. Russ.* **1915**, *47*, 805.

(30) Yamanaka, S.; Malla, P. B.; Komarneni, S. *J. Colloid Interface Sci.* **1990**, *134*, 51.

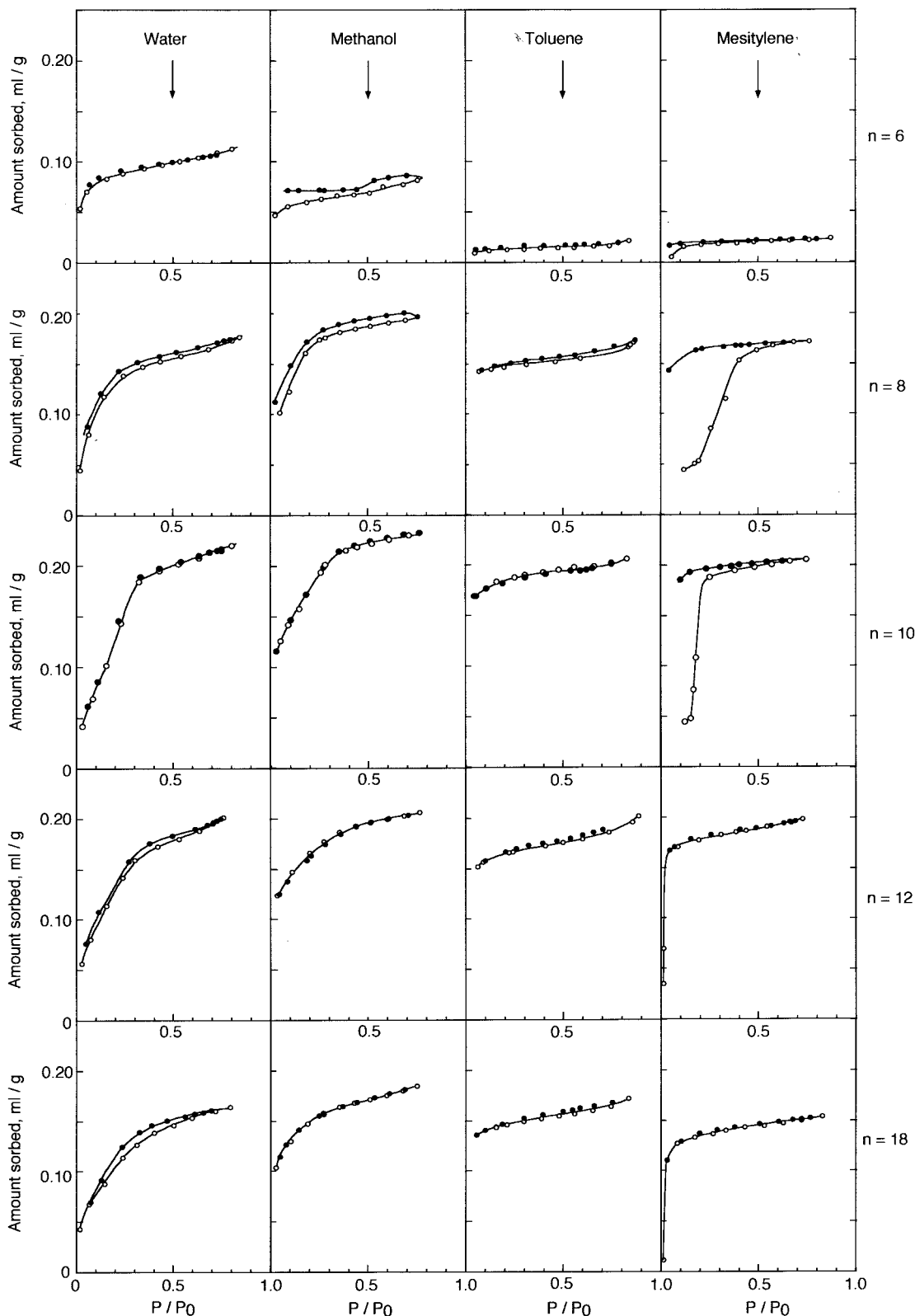
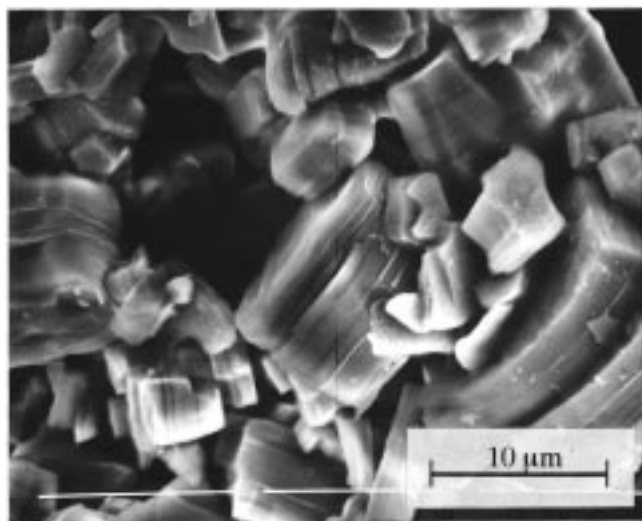


**Figure 7.** Adsorption (○)—desorption (●) isotherms for various vapors (water, methanol, toluene, and mesitylene) on the SiO<sub>2</sub>-MTO samples obtained by using different lengths of alkylammonium ions and calcined at 400 °C. The number of carbon atoms (*n*) in the alkyl chains are shown on the right-hand side. The columns and the lines of the figure compare the effects of the same kinds of vapors and alkyl chains, respectively.

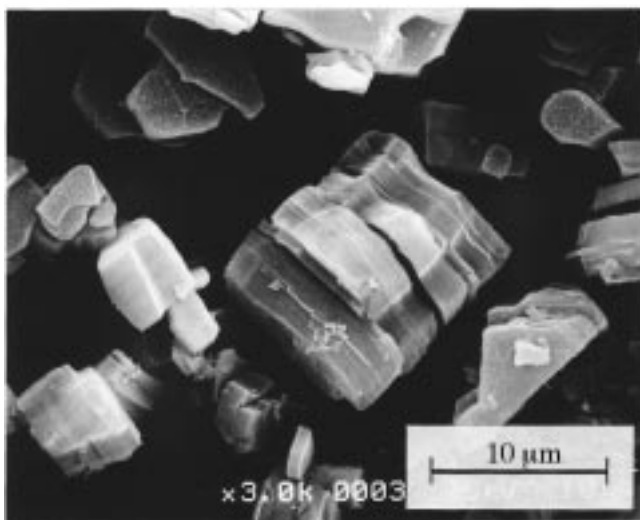
formed by the hydrolysis of TEOS in the interlayer space between the alkylammonium ions. The role of water should be carefully studied. It is interesting to note that the solids obtained in this study have micropores with little hysteresis, like zeolites. Gramlich and Meier<sup>31</sup> introduced the framework density (FD) to characterize

the void volume of zeolites, i.e., the number of tetrahedral units (SiO<sub>2</sub> and AlO<sub>2</sub> in zeolites) per nm<sup>3</sup>. The FD of the interlayer silica pillars was estimated from the

(31) Gramlich-Meier, R.; Meier, W. M. *J. Solid State Chem.* **1982**, *44*, 41.



(a)



(b)

**Figure 8.** SEM photographs of (TEOS) A<sub>10</sub>-MTO (a) and SiO<sub>2</sub>-MTO (b) obtained by calcination at 400 °C.

increase of the unit cell volumes and the amount of silica intercalated and are compared with those of some zeolites and silica polymorphs in Table 2. It is interesting that FD of silica pillars is comparable with those of faujasite and zeolite A, which have the smallest FD

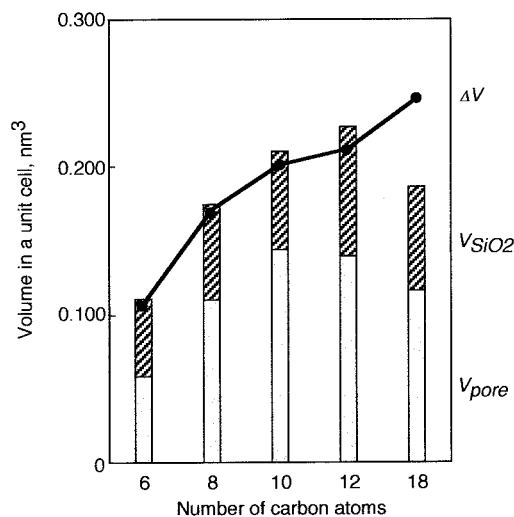


**Figure 9.** Volumes occupied by pores ( $V_{\text{pore}}$ ) and silica pillars ( $V_{\text{SiO}_2}$ ) in the unit cell as a function of the number of carbon atoms in the alkyl chains used. The increase of the unit cell volumes  $\Delta V$  (●) can be compared with the volume ( $V_{\text{pore}} + V_{\text{SiO}_2}$ ) by silica pillaring.

**Table 2. Framework Density (FD) of Silica Pillars between the Titanate Layers in Comparison with Those of Some Zeolites and Silica Polymorphs**

	FD		FD
silica pillar		zeolite A	12.9
$n^a = 6$	19.5	faujasite	12.7
$n = 8$	14.8	quartz	26.6
$n = 10$	12.9	crystalite	23.5
$n = 12$	17.6		
$n = 18$	10.4		

<sup>a</sup>  $n$  is the number of carbon atoms of the alkylammonium ions used for the silica pillaring.

among zeolites. The high surface area of the pillared titanates can be attributed to the low FD.

In our preliminary study, the silica pillared samples could be electrochemically reduced and oxidized. Microporous solids in which electron-transfer reactions will be possible for catalysis and battery electrodes should be of interest in the future.

**Acknowledgment.** This study has been supported by Grant-in-Aid for Scientific Research (B) from the Ministry of Education, Science, Sports and Culture, Japan.

CM980099X